

SUPPLEMENTARY INFORMATION

Tailoring shell thickness of yolk-shell structured carbon microspheres : applications in metal selenide and carbon composite microspheres for enhanced sodium ion properties

Hyo Yeong Seo,^{‡^a} Jae Hyeon Choi,^{‡^a} Yeong Beom Kim,^{ac} Jung Sang Cho,^{*^b} Yun Chan Kang,^{*^c} and Gi Dae Park^{*^a}

^aDepartment of Advanced Materials Engineering, Chungbuk National University, Chungdae-ro 1, Seowon-Gu, Cheongju, Chungbuk 28644, Republic of Korea, E-mail: gdpark@chungbuk.ac.kr; Fax: (+82) 43-271-3222

^bDepartment of Engineering Chemistry, Chungbuk National University, Chungdae-ro 1, Seowon-Gu, Cheongju, Chungbuk 28644, Republic of Korea, E-mail: jscho@cbnu.ac.kr; Fax: (+82) 43-262-2380

^cDepartment of Materials Science and Engineering, Korea University, Anam-Dong, Seongbuk-Gu, Seoul 136-713, Republic of Korea, E-mail: yckang@korea.ac.kr; Fax: (+82) 2-928-3584

[‡] These authors contributed equally to this work.

Materials Characterizations

The morphological characteristics of the samples were investigated via scanning electron microscopy (SEM, VEGA3) and field emission-transmission electron microscopy (FE-TEM, JEM-2100F) at the Korea Basic Science Institute (Daegu). The crystal structures of the samples were analyzed using X-ray diffraction spectroscopy (XRD, X'Pert PRO with Cu K α radiation, $\lambda = 1.5418 \text{ \AA}$). X-ray photoelectron spectroscopy (XPS) of the samples was performed using ESCALAB-250 with Al K α radiation (1486.6 eV). Thermogravimetric (TG) analysis (Pyris 1 Thermogravimetric Analyzer, PerkinElmer) was conducted in the range 25–800 °C at 10 °C min⁻¹ under an air atmosphere. The surface area and porosities of the samples were analyzed via Brunauer–Emmett–Teller (BET) method, using high-purity N₂. The structural characteristics of carbon in the sample were investigated via Raman spectroscopy (Jobin Yvon LabRam HR800, excited by a 632.8-nm He/Ne laser) at room temperature.

Electrochemical Measurements

To measure the electrochemical properties of the samples for SIBs, a 2032-type coin cell constructed from electrodes prepared via the slurry process was utilized. For the anode electrode, the active materials, carbon black (Super-P), and sodium carboxymethyl cellulose (CMC) in a weight ratio of 7:2:1 were uniformly mixed with water solvent in a mortar. The well-mixed slurry was coated onto Cu foil using a doctor blade and dried in a vacuum oven for 3 h. Sodium metal and a microporous polypropylene film were used as the counter electrode and separator, respectively. The electrolyte for SIBs was 1M NaClO₄ dissolved in ethylene carbonate/dimethyl carbonate (1/1 v/v). The diameter and mass loading of the negative electrode were 14 mm and 1.4 mg cm⁻², respectively. The discharge–charge characteristics of the samples were analyzed via cycling in 0.001–3.0 V potential range at various current densities. Cyclic voltammetry (CV) analysis was conducted at a scan rate of 0.1 mV s⁻¹. Electrochemical impedance spectroscopy (EIS, ZIVE SP1) measurements of the electrode were performed over a frequency range of 0.01 Hz – 100 kHz. In-situ EIS analysis was performed at preselected potentials during the discharge and charge process at a current density of 0.1 A g⁻¹. Galvanostatic intermittent titration (GITT) measurements were performed at a constant current density of 0.1 A g⁻¹ with a current pulse duration of 20 min and relaxation time of 60 min.

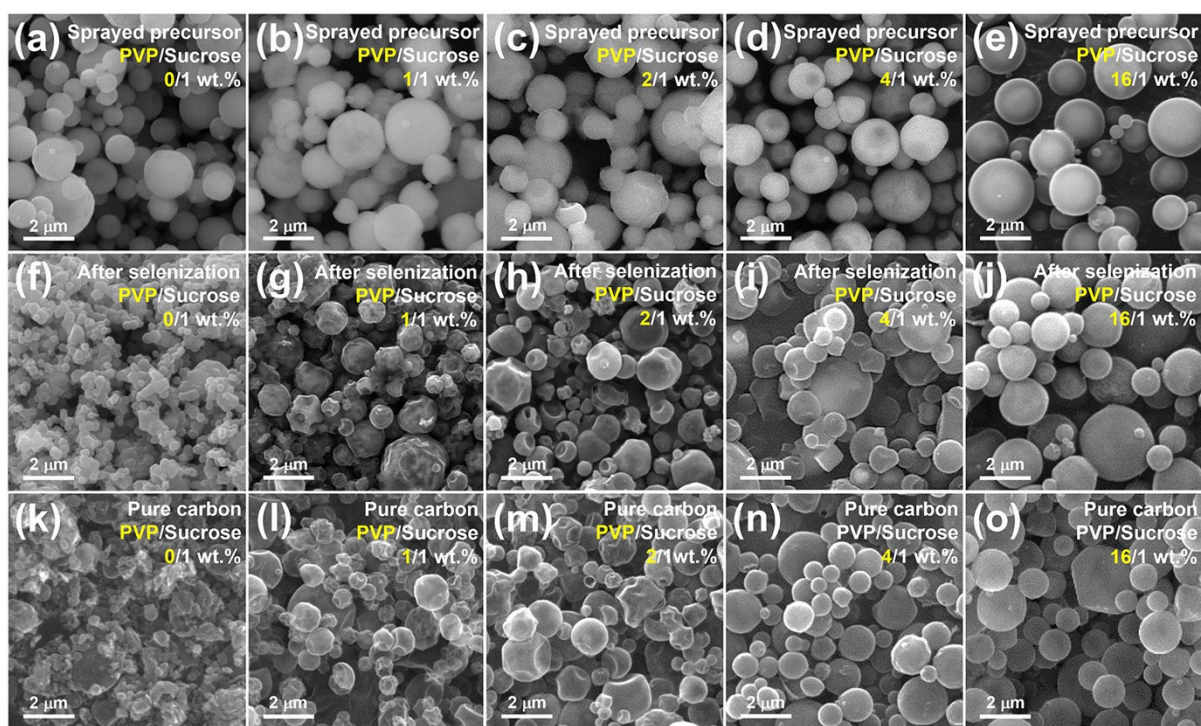


Fig. S1 SEM images of (a-e) spray pyrolyzed precursor with different ratio of PVP/sucrose, (f-j) MgO-MgSe-C@C obtained after selenization of precursor, and (k-o) carbon yolk-shell obtained after etching process: (a, f and k) PVP/sucrose 0/1 wt%, (b, g and l) PVP/sucrose 1/1 wt%, (c, h and m) PVP/sucrose 2/1 wt%, (d, i and n) PVP/sucrose 4/1 wt%, and (e, j and o) PVP/sucrose 16/1 wt%.

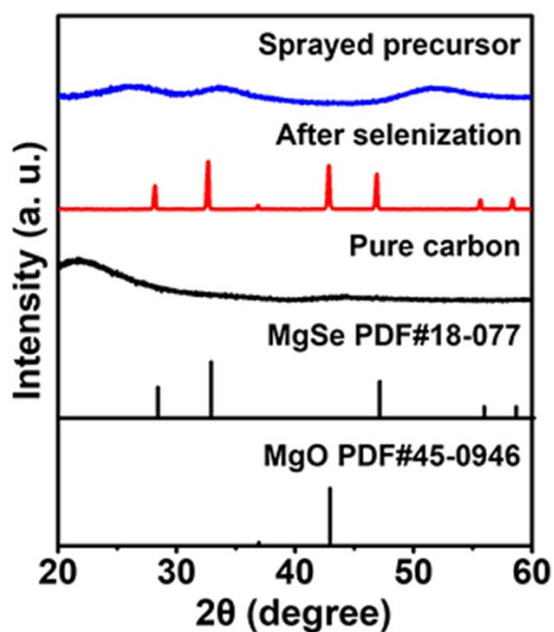


Fig. S2 XRD patterns of spray pyrolyzed precursor, post treated MgO-MgSe-C@C microsphere, after etched C-YS 2/1 microsphere from spray solution containing Sn oxalate, Mg nitrate, sucrose and PVP.

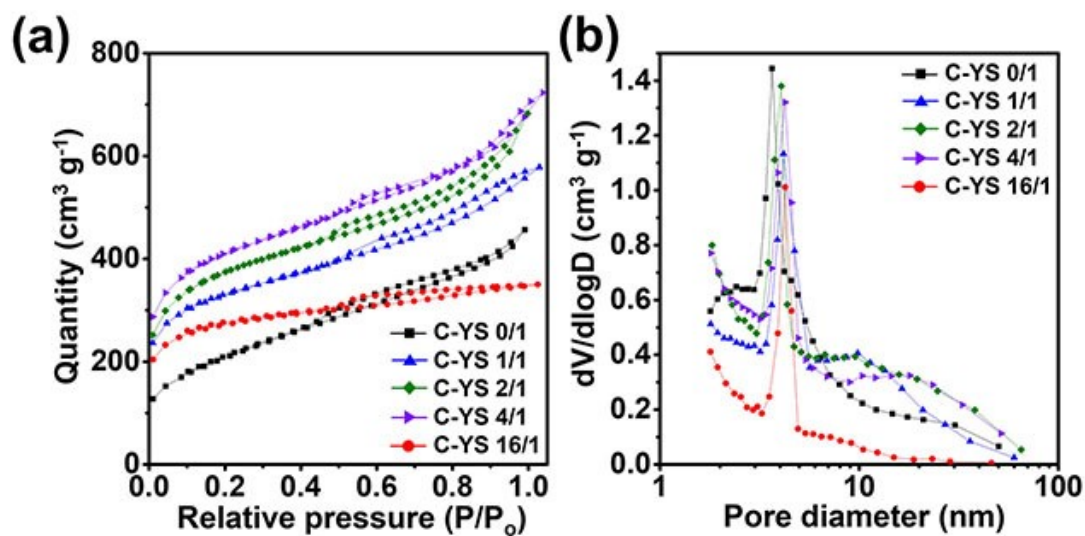


Fig. S3 (a) N_2 gas adsorption and desorption isotherms and (b) BJH pore-size distribution of carbon yolk-shell microspheres with different ratio of PVP/sucrose.

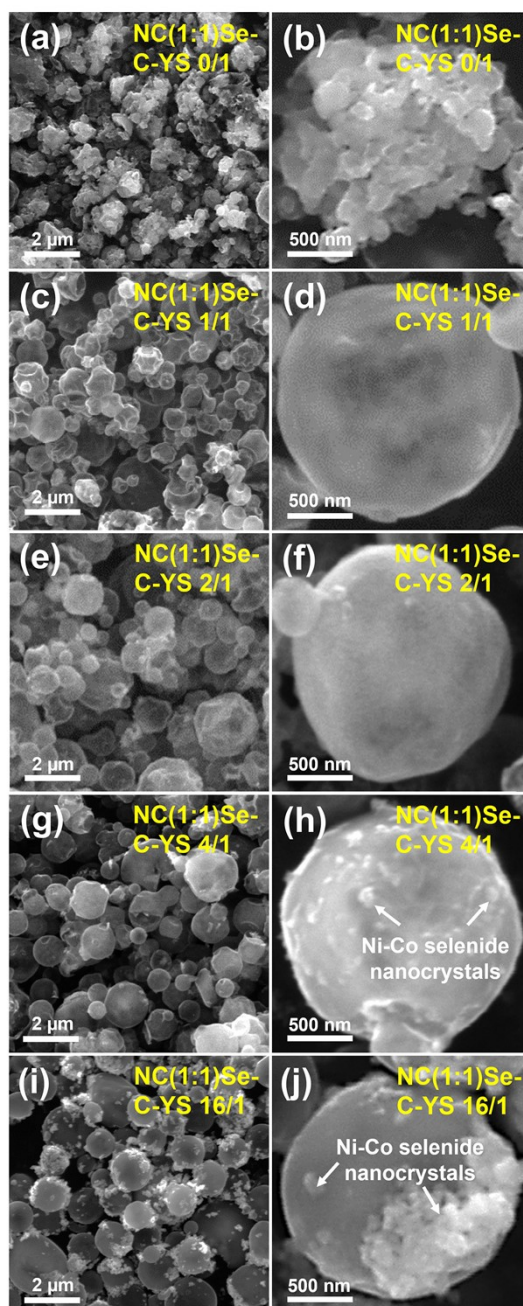


Fig. S4 SEM images of NC(1:1)Se-C-YS with different ratio of PVP/sucrose: (a and b) NC(1:1)Se-C-YS 0/1, (c and d) NC(1:1)Se-C-YS 1/1, (e and f) NC(1:1)Se-C-YS 2/1, (g and h) NC(1:1)Se-C-YS 4/1, and (i and j) NC(1:1)Se-C-YS 16/1.

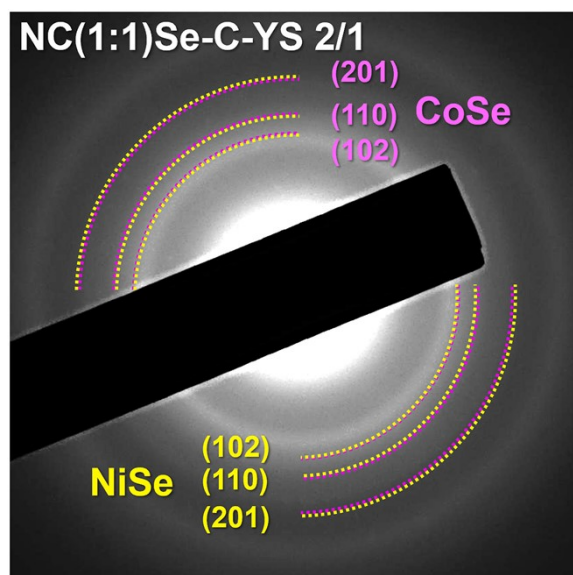


Fig. S5 SAED patterns of NC(1:1)Se-C-YS 2/1.

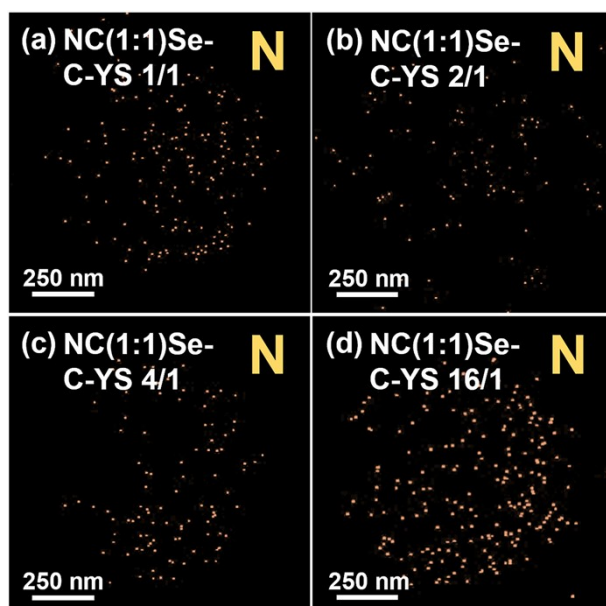


Fig. S6 Mapping images of N: (a) NC(1:1)Se-C-YS 1/1, (b) NC(1:1)Se-C-YS 2/1, (c) NC(1:1)Se-C-YS 4/1, and (d) NC(1:1)Se-C-YS 16/1.

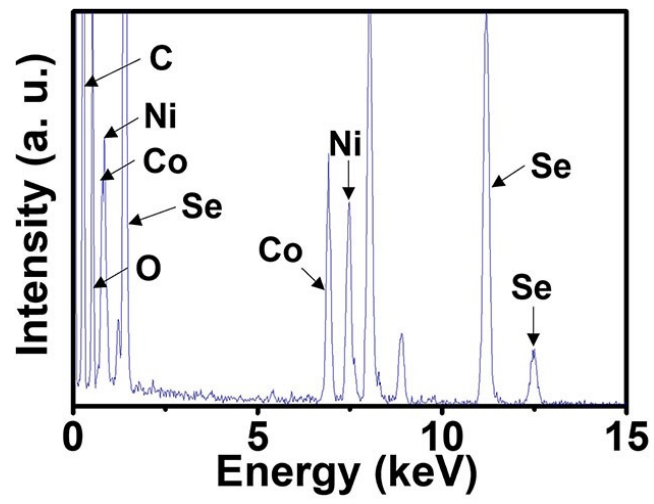


Fig. S7 EDS spectrum of NC(1:1)Se-C-YS 2/1.

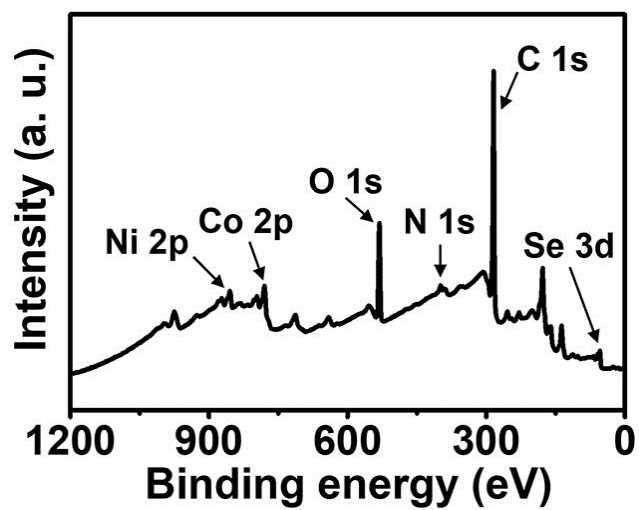


Fig. S8 XPS survey spectrum of NC(1:1)Se-C-YS 2/1.

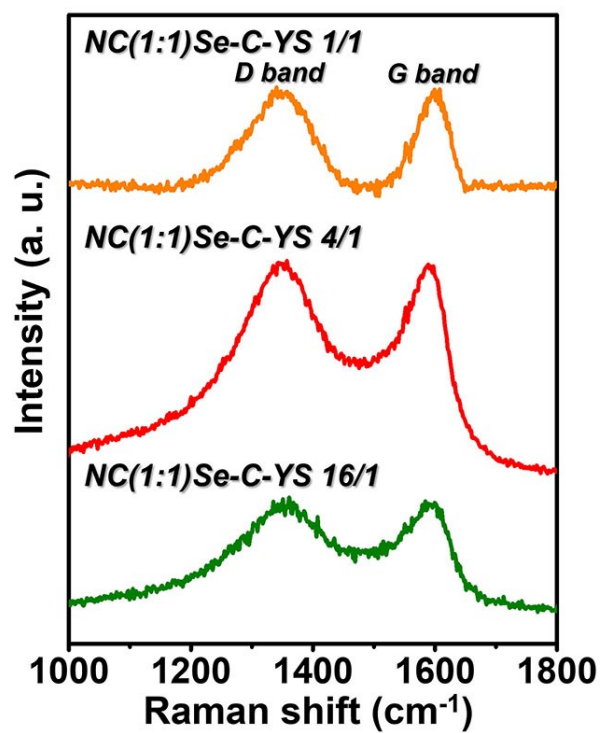


Fig. S9 Raman spectra of NC(1:1)Se-C-YS 1/1, NC(1:1)Se-C-YS 4/1, and NC(1:1)Se-C-YS 16/1.

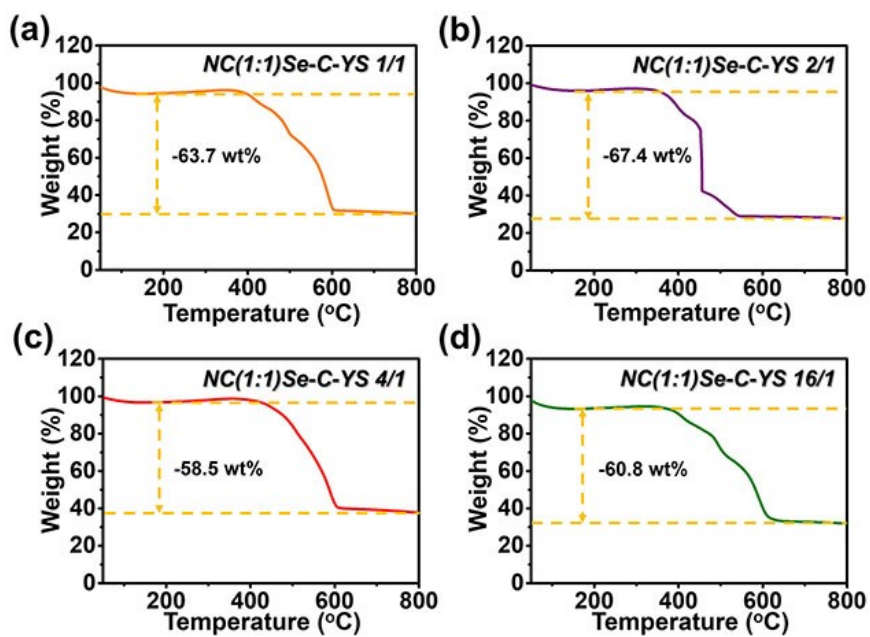


Fig. S10 TG curves of (a) NC(1:1)Se-C-YS 1/1, (b) NC(1:1)Se-C-YS 2/1, (c) NC(1:1)Se-C-YS 4/1 and (d) NC(1:1)Se-C-YS 16/1.

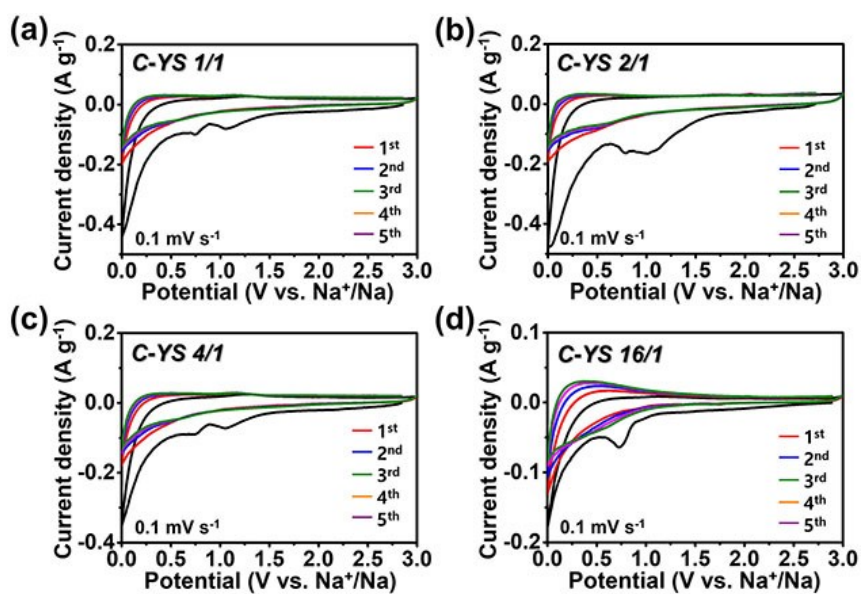


Fig. S11 CV curves of (a) C-YS 1/1, (b) C-YS 2/1, (c) C-YS 4/1, and (d) C-YS 16/1.

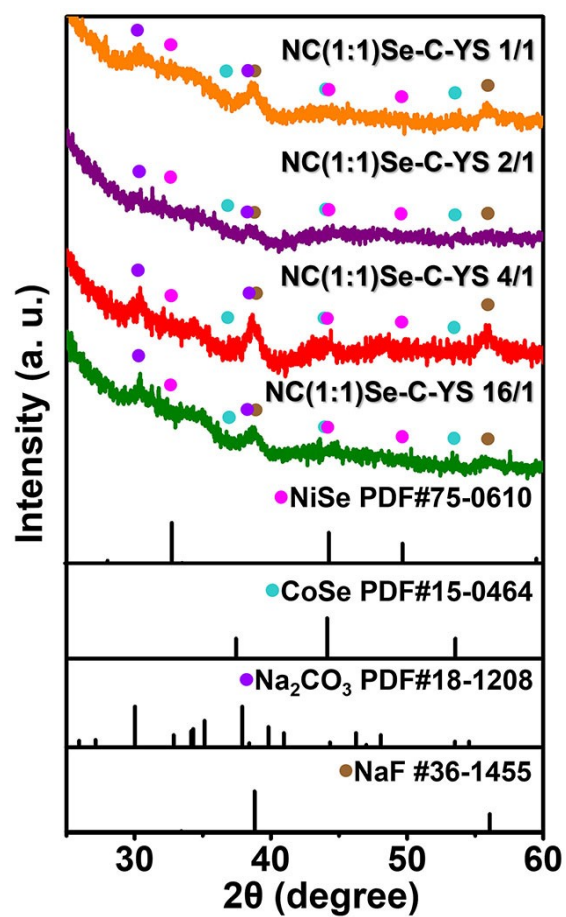


Fig. S12 XRD patterns of NC(1:1)Se-C-YS 1/1, NC(1:1)Se-C-YS 2/1, NC(1:1)Se-C-YS 4/1 and NC(1:1)Se-C-YS 16/1 electrode obtained after 100 cycles.

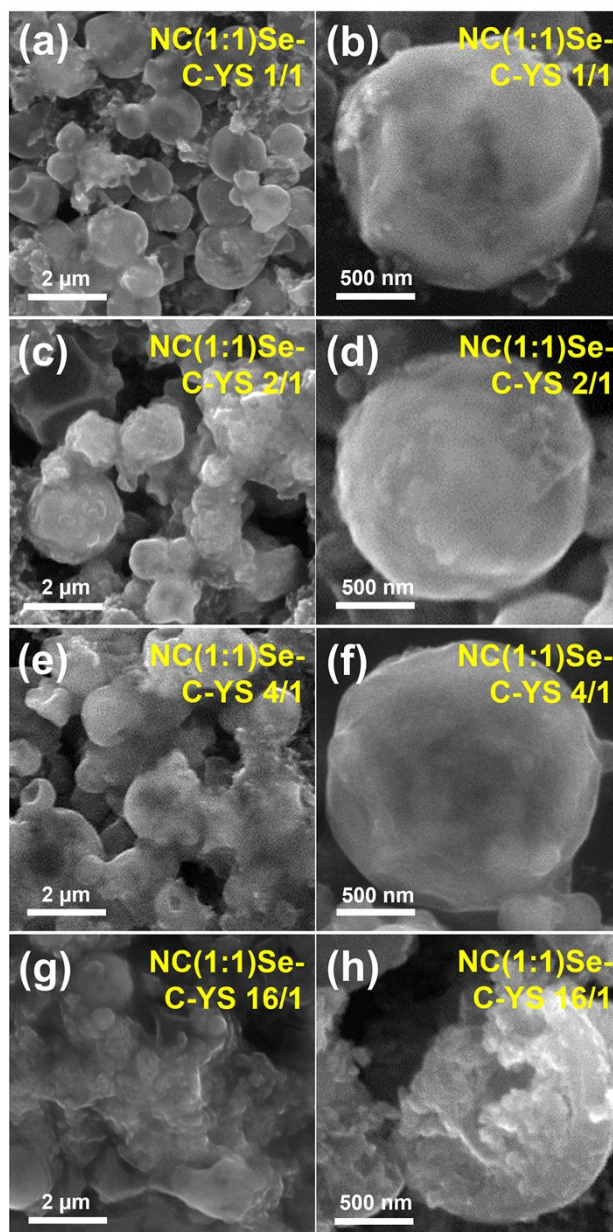


Fig. S13 SEM images after 100 cycles of (a and b) NC(1:1)Se-C-YS 1/1, (c and d) NC(1:1)Se-C-YS 2/1, (e and f) NC(1:1)Se-C-YS 4/1, and (g and h) NC(1:1)Se-C-YS 16/1.

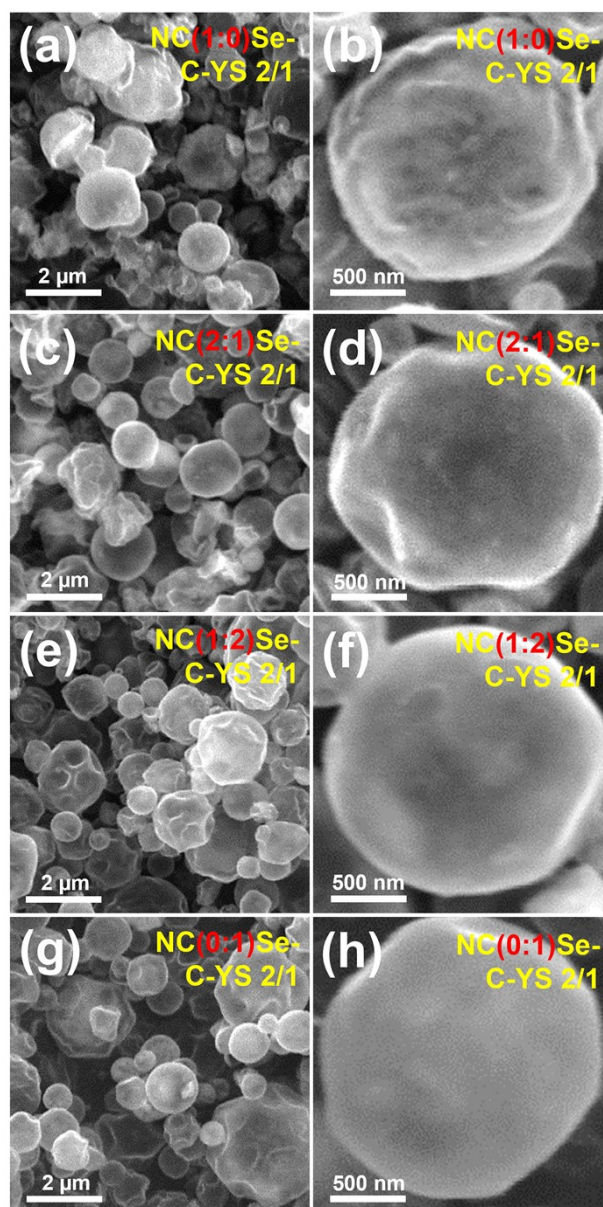


Fig. S14 SEM images of (a and b) NC(1:0)Se-C-YS 2/1, (c and d) NC(2:1)Se-C-YS 2/1, (e and f) NC(1:2)Se-C-YS 2/1, (g and h) and NC(0:1)Se-C-YS 2/1.

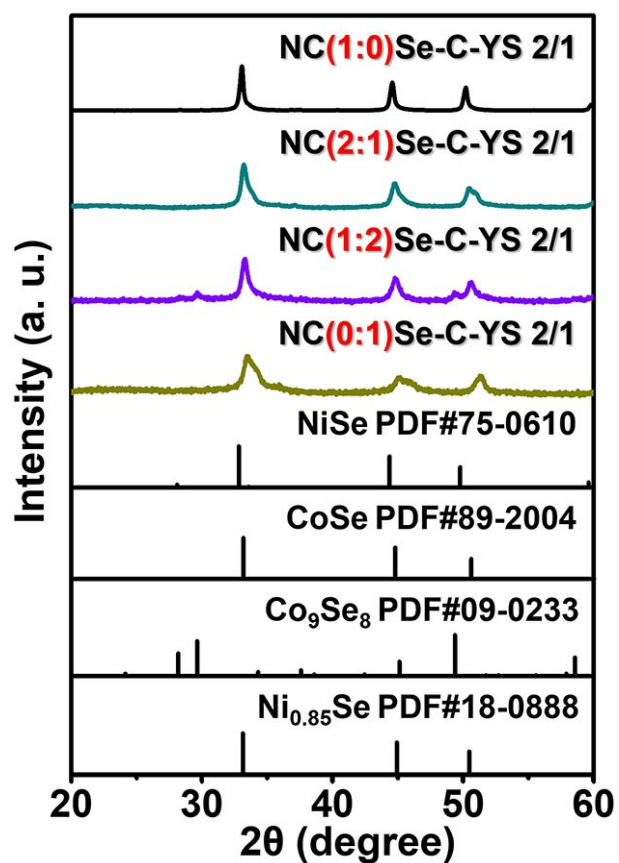


Fig. S15 XRD patterns of four nickel-cobalt selenide carbon yolk-shell microspheres with different ratios of Ni and Co: NC(1:0)Se-C-YS 2/1, NC(2:1)Se-C-YS 2/1, NC(1:2)Se-C-YS 2/1, and NC(0:1)Se-C-YS 2/1.

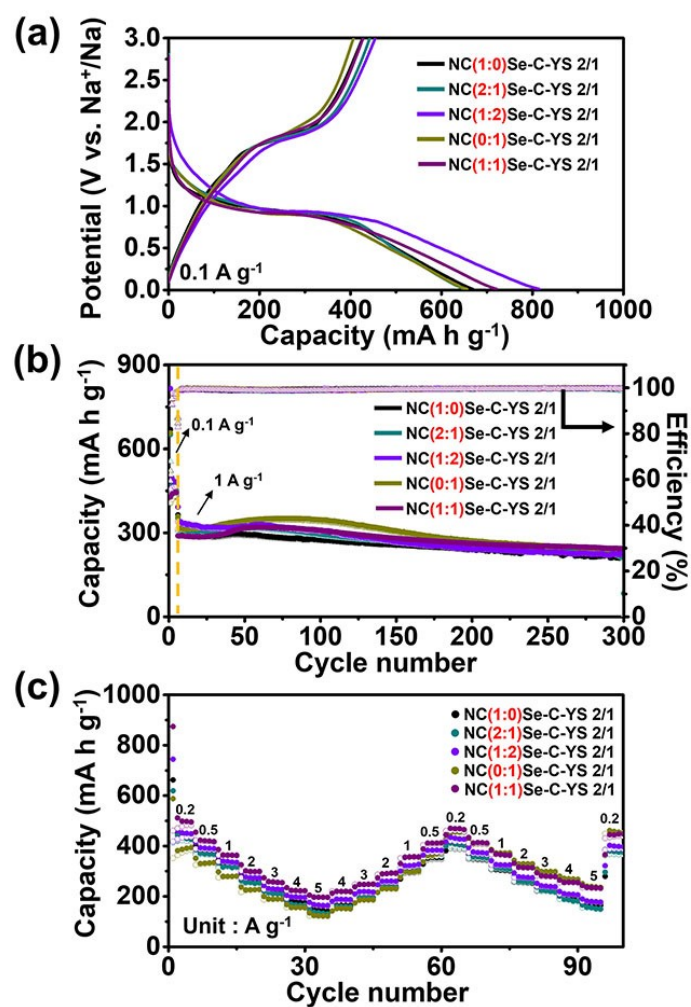


Fig. S16 Electrochemical properties of NC(1:0)Se-C-YS 2/1, NC(2:1)Se-C-YS 2/1, NC(1:1)Se-C-YS 2/1, NC(1:2)Se-C-YS 2/1, and NC(0:1)Se-C-YS 2/1: (a) initial discharge and charge curves, (b) cyclic performances at a current density of 1 A g^{-1} after the initial 5 cycles at 0.1 A g^{-1} and (c) triplicate evaluations of rate performances from 0.2 to 5 A g^{-1} .

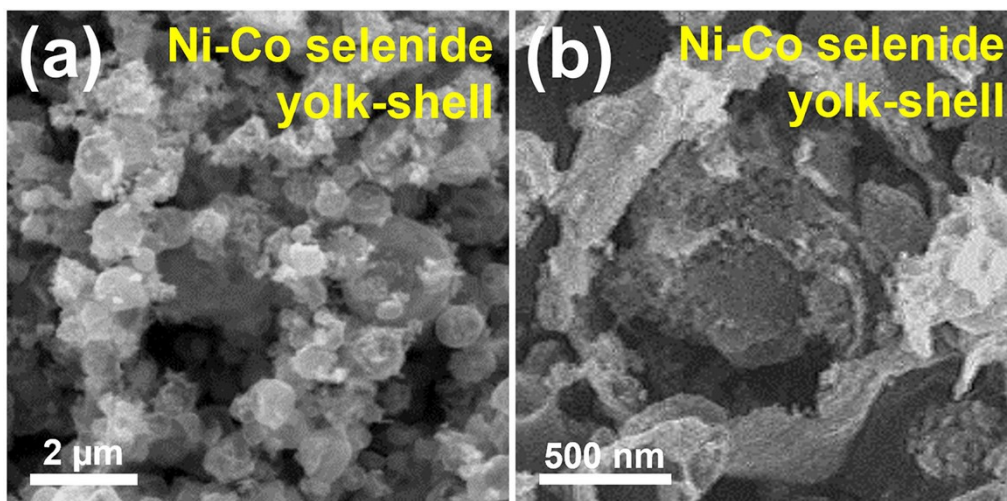


Fig. S17 SEM images of nickel-cobalt selenide yolk-shell.

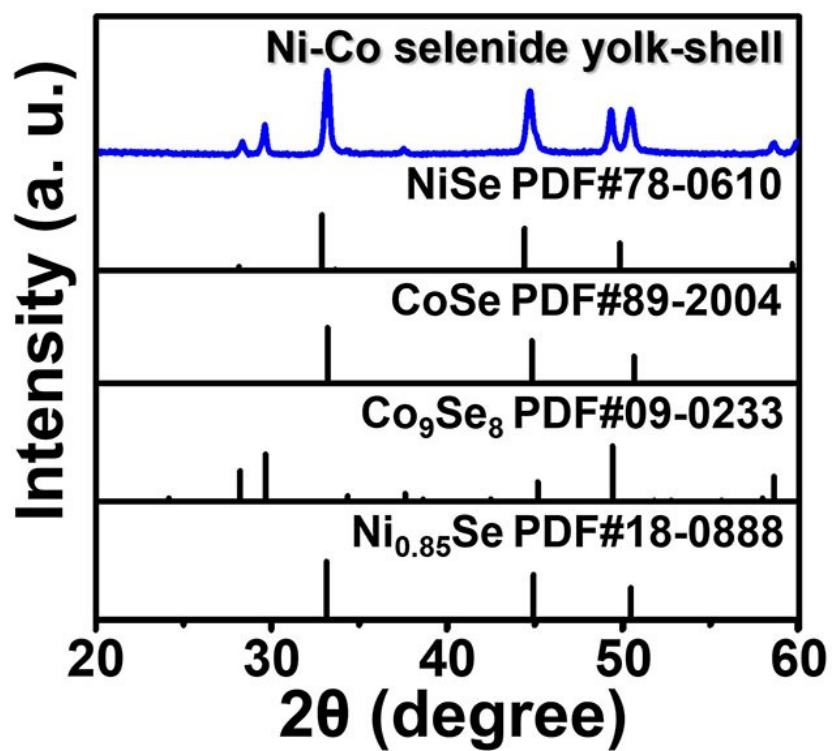


Fig. S18 XRD pattern of nickel-cobalt selenide yolk-shell.

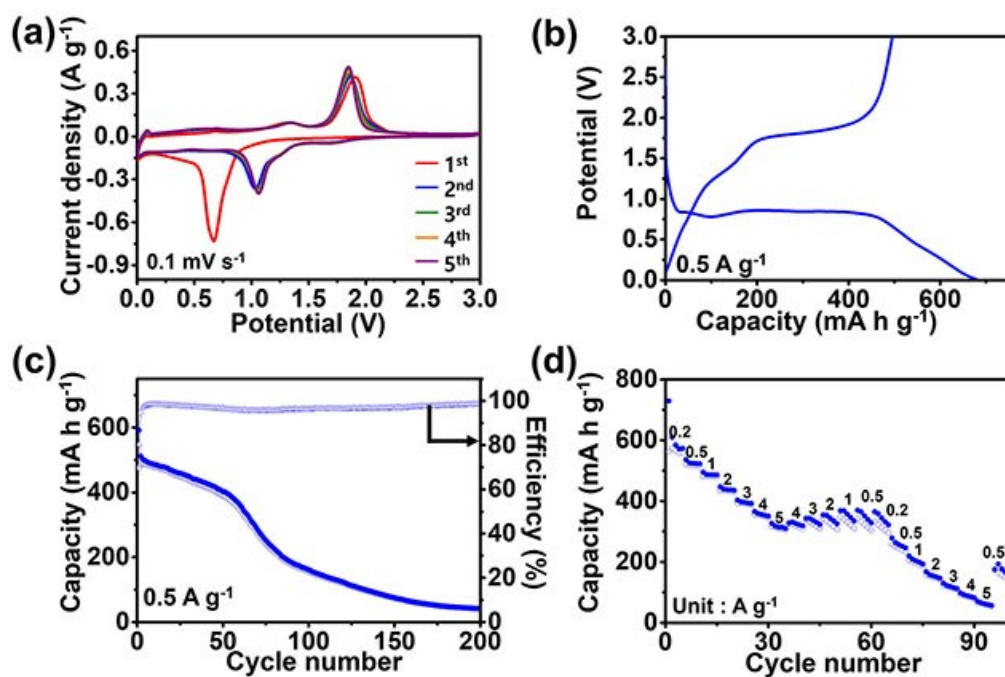


Fig. S19 Electrochemical properties of nickel-cobalt selenide yolk-shell for SIBs. (a) CV curves, (b) initial discharge and charge curves, (c) cycle performance at a current density of 0.5 A g⁻¹, and (d) rate performances.

Table. S1 Weight percentage of elements based on the EDS spectrum of NC(1:1)Se-C-YS
2/1.

Element	Line Type	k Factor	Absorption Correction	Wt%
C	K series	2.773	1.00	51.10
O	K series	2.029	1.00	8.81
Co	K series	1.173	1.00	7.91
Ni	K series	1.145	1.00	7.99
Se	K series	1.607	1.00	24.2
Total				100.00

Table. S2 Comparison of electrochemical performances of various nickel-cobalt selenide-C anode materials for SIBs reported in the previous literatures.

Electrode material	Preparation method	Cyclic performance (mA h g ⁻¹) {cycle #} [current density (A g ⁻¹)]	Rate performance (mA h g ⁻¹) [current density (A g ⁻¹)]	Potential range [V]	Ref.
NC(1:1)Se-C-YS 2/1	Metal salt infiltration + selenization	342.4 {200} [0.5]	198.5 [5.0]	0.001-3.0	Our work
Co-Ni-Se/BWCF-160	Microwave precipitation + ion exchange + chemical etching + hydrothermal selenization	403 {100} [0.1]	211 [1.0]	0.01-3.0	S1
NiCoSe ₂ @C	Hydrothermal method + dopamine coating + carbonization	370.56 {100} [0.1]	252.3 [5.0]	0.5-2.8	S2
NiCo ₂ Se ₄	Solvothermal method	284 {200} [1.0]	220 [5.0]	0.4-2.9	S3
NiCoSe _x /CG	Hydrothermal method + selenization	206.8 {100} [0.1]	140 [5.0]	0.5-2.9	S4
Ni ₃ Se ₄ @CoSe ₂ @C/CNTs	Precipitation (MOF) + selenization	295 {300} [0.5]	200 [3.0]	0.01-3.0	S5
CoSe ₂ /NiSe ₂ @NC-CNT	Wet-chemistry approach + selenization	305 {300} [0.1]	289 [5.0]	0.01-3.0	S6
MNCS50	Solvothermal method	473 {60} [0.05]	293 [1.0]	0.01-3.0	S7
NiCo ₂ Se ₄ @NPC	Precipitation (MOF) + selenization	462.14 {70} [0.1]	371.3 [2.0]	0.01-3.0	S8

- S1 M. Gao, Y. Xue, Y. Zhang, C. Zhu, H. Yu, X. Guo, S. Sun, S. Xiong, Q. Kong and J. Zhang, Growing Co–Ni–Se nanosheets on 3D carbon frameworks as advanced dual functional electrodes for supercapacitors and sodium ion batteries, *Inorg. Chem. Front.*, 2022, **9**(15), 3933-3942.
- S2 Y.-H. Zhang, J.-L. Wang, H.-Y. Yan, J.-T. Zhao, D.-D. Wang, S.-H. Luo, Q. Wang and X. Liu, Short rod-like NiCoSe₂ binary-metal selenide nanomaterials of carbon-coated as high-performance anode for sodium-ion batteries, *Ionics*, 2023, 1-11.
- S3 W. Zhong, Q. Ma, W. Tang, Y. Wu, W. Gao, Q. Yang, J. Yang and M. Xu, Construction of a bimetallic nickel–cobalt selenide pompon used as a superior anode material for high performance sodium storage, *Inorg. Chem. Front.*, 2020, **7**(4), 1003-1011.
- S4 D. Li, H. Liu, H. Liu, Y. Chen, C. Wang and L. Guo, A NiCoSe_x/CG heterostructure with strong interfacial interaction showing rapid diffusion kinetics as a flexible anode for high-rate sodium storage, *Dalton Trans.*, 2023, **52**(16), 5192-5201.
- S5 H. Zhu, Z. Li, F. Xu, Z. Qin, R. Sun, C. Wang, S. Lu, Y. Zhang and H. Fan, Ni₃Se₄@CoSe₂ hetero-nanocrystals encapsulated into CNT-porous carbon interpenetrating frameworks for high-performance sodium ion battery, *J. Colloid Interface Sci.*, 2022, **611**, 718-725.
- S6 S. Chen, H. Ma, X. Zhou, D. Jin, J. Yan, G. Wang, W. Zhao, J. Yun, H. Zhang and Z. Zhang, Heterostructure Interface Construction of Cobalt/Nickel Diselenides Hybridized with sp²–sp³ Bonded Carbon to Boost Internal/External Sodium and Potassium Storage Dynamics, *ACS Appl. Energy Mater.*, 2022, **6**(1), 424-438.
- S7 P. Santhoshkumar, N. Shaji, G. S. Sim, M. Nanthagopal, J. W. Park and C. W. Lee, Facile and solvothermal synthesis of rationally designed mesoporous NiCoSe₂ nanostructure and its improved lithium and sodium storage properties, *Appl. Mater. Today*, 2020, **21**, 100807.
- S8 L. Li, J. Zhao, Y. Zhu, X. Pan, H. Wang and J. Xu, Bimetallic Ni/Co-ZIF-67 derived NiCo₂Se₄/N-doped porous carbon nanocubes with excellent sodium storage performance, *Electrochim. Acta*, 2020, **353**, 136532.